

Our measurements have been plagued by lack of reproducibility of the probe signals. This (together with a lack of understanding of the behavior of probes in a magnetic field) has restricted us in having to rely on the first arriving probe signal for quantitative data. Even this is not as reproducible as would be desired. This can be seen from the relatively large spread of the points about the experimental curves. Apparently, the way in which the source fires is sensitive to a number of factors which at present are uncontrollable.

At present we have only crude estimates of the number of ions emitted from the source and the composition of the resulting plasma (i.e., percentages of deuterium and titanium ions). We do not even know to what extent the many phenomena observed are peculiar to the titanium-deuterium source. A few experiments have been done with sources constructed from other electrode materials, but much further work needs to be done.

One experimental parameter which has not been varied in our experiments is the pressure of the residual gas. In the range of pressures (about 10^{-6} mm Hg) at which the experiments reported here were done, the residual gas is expected to have a negligible influence. At higher pressures (about 10^{-3} mm Hg) quite different phenomena have been observed. It would be of interest to extend the velocity measurements into the range of higher pressures.

ACKNOWLEDGMENTS

The authors wish to acknowledge the interest and support in this work of S. A. Colgate and C. M. Van Atta and to thank O. A. Twite for his invaluable aid in performing the experiments; E. Harris and R. Theus are especially grateful for the warm hospitality extended them during their stay at the University of California Radiation Laboratory.

Paramagnetic Resonance of Free Radicals at Millimeter Wave Frequencies*

AREND VAN ROGGEN, LIEN VAN ROGGEN, AND WALTER GORDY
Department of Physics, Duke University, Durham, North Carolina

(Received September 21, 1956)

Paramagnetic resonance experiments have been made at 36 kMc/sec and at 75 kMc/sec on single crystals and on solid and liquid solutions of the free radicals: diphenyl picryl hydrazyl (DPPH), *p*-anisyl nitrogen oxide, and 2-(phenyl nitrogen oxide)-2-methyl pentane-4-one-oxime-*N*-phenyl ether. The measurements indicate fields axially symmetric about the paramagnetic element in the first two, with $g_{\parallel}=3.0035$, $g_{\perp}=2.0043$ for the first and $g_{\parallel}=2.0095$, $g_{\perp}=2.0035$ for the second. The third radical has a lower symmetry with $g_x=2.0042$, $g_y=2.0064$, and $g_z=2.0083$ along the principal axes of susceptibility. The hyperfine structure of DPPH in dilute solution (earlier observed by others) consists of

five components, arising from interactions with the two N^{14} nuclei of the N^{14} group. The other two radicals of the present study were found to have in dilute liquid solution a triplet hyperfine structure arising from interaction with a single N^{14} nucleus. This structure is interpreted as indicating that the odd electron is localized mainly on an $-N=O$ group in each radical. The anisotropies in the g factors are believed to arise mainly from a residual spin-orbit coupling. A sensitive millimeter-wave magnetic-resonance spectrometer employing superheterodyne detection with a crystal multiplier as the beat frequency oscillator is described.

INTRODUCTION

PARAMAGNETIC resonance measurements at millimeter-wave frequencies have certain advantages over those at lower frequencies. Because of the commensurately higher magnetic fields at the higher frequencies, the field-dependent components of the resonance are more widely separated. When there are in the sample two radicals with g factors differing only slightly, the resonances might overlap at the lower fields and be resolved at the higher ones. From the resonance condition, $h\nu=g\beta H$, it follows that when the observation frequency is held constant two components with g factors differing by a small Δg will occur at fields differing by:

$$\Delta H = (\Delta g/g)H = (\Delta g/g)(h\nu/g\beta), \quad (1)$$

if g is independent of H , as is found true for the radicals under investigation. Whenever ΔH is measurable at different frequencies, the higher the observation frequency the smaller is the Δg which can be detected and the more accurately a given Δg can be measured.

One of the three free radicals included in the present study, diphenyl picryl hydrazyl (DPPH), has already been investigated rather thoroughly in the lower centimeter-wave region. The resonance of this radical was first detected by Holden, Kittel, Merritt, and Yager.¹ Later it was found to have an N^{14} hyperfine structure in dilute solution by Hutchison, Pastor, and Kowalsky,² who also made measurements on single crystals and showed that the g factor is not exactly

¹ Holden, Kittel, Merritt, and Yager, *Phys. Rev.* **75**, 1614 (1949); **77**, 147 (1950).

² Hutchison, Pastor, and Kowalsky, *J. Chem. Phys.* **20**, 534 (1952).

* This work has been supported by a contract with the Office of Ordnance Research, Department of the Army.

isotropic but varies from 2.0035 to 2.0041 depending upon the orientation of the crystal in the magnetic field. This latter observation, made at 23 kMc/sec, was later confirmed at the same frequency by Kikuchi and Cohen,³ who found a similar and somewhat larger anisotropy in the picryl *n*-amino carbazyl radical. Dr. Kikuchi suggested that we include single crystals of DPPH in the present study and kindly supplied us with a sample of the radical. More recently Livingston and Zeldes⁴ have found that the line width as well as the *g* factor for single crystals of DPPH has a slight orientation-dependence. The other two radicals included in the present study (see Table I) have not been so thoroughly investigated as DPPH although their resonance in the powder form has been previously detected.¹

EXPERIMENTAL ASPECTS

In general, the apparatus used for paramagnetic resonance absorption consist of a microwave power source, a measuring cell (cavity), and a microwave detector, followed by electronic devices that either display the resonance curve directly or record its derivative on a chart. Bolometer detection was employed in our measurements in the wavelength range above 5 mm (frequencies below 60 kMc). In the 3- to 5-mm wavelength range, however, we were able to achieve the best sensitivity with superheterodyne detection. Insufficient power is available in this range for operation of a spectrometer of high sensitivity with bolometer detection, yet enough is available for generation of excessive low-frequency noise in the simple, crystal video spectrometers. Superheterodyne detection avoids the low-frequency noise in crystals by making possible amplification of the signal at high i.f. frequencies. In a magnetic resonance spectrometer for which it is not necessary to vary the observation frequency in the search for the resonance, such detection presents no particular difficulties.

A block diagram of our 3-5 mm wave magnetic resonance spectrometer is given in Fig. 1. It employs a crystal multiplier for beat oscillator as well as for signal power. The signal source is a 1N53 Sylvania crystal which generates harmonic power from the fundamental power of a Raytheon 2K33 klystron. The multiplier in which the crystal is mounted is tuned for optimum output energy in the third harmonic. Another 1N53 crystal serves as local oscillator and mixer detector. This crystal is mounted in an equivalent multiplier with an additional connection for a coaxial output of the rectified crystal current. This multiplier is fed by a second 2K33 klystron. Microwave energy from the first multiplier passes a tuned, resonant cavity and mixes in the second multiplier to form a 30-Mc/sec beat, which is brought out via a coaxial cable into an i.f. amplifier with a 3- to 4-Mc/sec band width at 30 Mc/sec.

³ C. Kikuchi and V. W. Cohen, *Phys. Rev.* **93**, 394 (1954).

⁴ R. Livingston and H. Zeldes, *J. Chem. Phys.* **24**, 170 (1956).

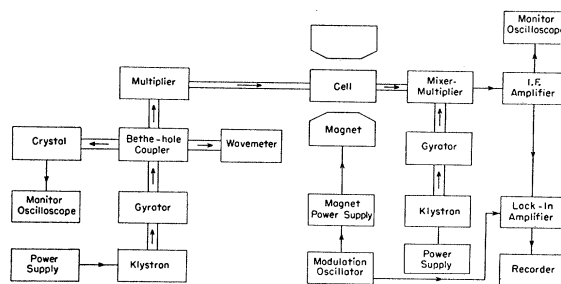


FIG. 1. Diagram of millimeter-wave magnetic resonance spectrometer.

Changes in absorption in the sample cavity are reproduced as amplitude modulation of the i.f. output. In a measurement, the magnetic field is varied at a constant rate by a synchronous motor, and in addition a small 16-cps sine-wave modulation is continuously applied to the field. When the magnetic field reaches the proper value for resonance absorption, the rectified output from the i.f. strip consists of a 16-cps sine wave, the amplitude of which is proportional to the derivative of the absorption curve. This i.f. output is amplified again in a narrow-band audio amplifier, tuned with a twin-T to 16 cps, and is then fed into a lock-in detector. The final output is displayed on a direct current recorder which shows the derivative of the absorption plotted against the magnetic field.

With such a spectrometer, considerable care must be taken to keep the frequency drift and instability small. The klystrons were water-cooled and heat-insulated, and the whole system was rigidly mounted. Even so, the beat note was not sufficiently constant to remain during a measurement within the 3-Mc band-width of the i.f. amplifier. Frequency drifts resulted in spurious noise. Such drift effects can be eliminated by electronic stabilization of the oscillator frequencies or by locking the two oscillators together. However, a simpler, more convenient method was found to reduce the drift noise greatly: the source klystron was subjected to a saw-tooth frequency modulation of 180 cps so as to sweep its frequency periodically through the response range of the mixer. Although the signal was reduced by this modulation, the drift noise was so much more decreased that the over-all signal-to-noise ratio was greatly improved. The audio amplifier was not blocked by the 180-cps sweep since it passed only in the 16-cps region where, obviously, no harmonics from the sweep occur. The output from the i.f. strip was displayed on the monitor oscilloscope, which does not respond to the broader cavity resonance. This monitor was used as a check on tuning conditions. To facilitate tuning, another monitor oscilloscope was made to display the energy mode of the signal klystron. Power for this monitor was fed out of the wave guide by means of a Bethe-hole coupler and was detected by a 1N23 crystal. Frequency measurements were made in the usual manner. The

mixer-multiplier had a crystal current meter (built into the i.f. amplifier circuit) that allowed reading of optimum working current.

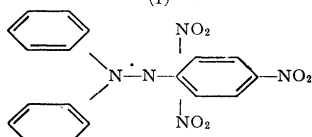
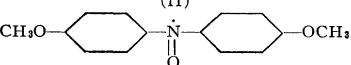
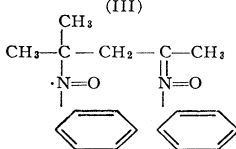
The cavity was of the right cylindrical type, oscillating in the TE_{01n} mode. It was of the transmission type, having two coupling irises to connect it with the input and output wave guide. The cavity was tunable with a plunger and had in the opposite end-plate a centered hole through which the sample could be inserted.

The magnetic field strength necessary for resonance at 75 kMc/sec is about 27 kilogauss, if one assumes a g value of approximately 2.0. This field was made with a 12-inch Varian magnet by use of special tapered pole pieces. The resulting homogeneity was not good, however. The apparent line width is a function of sample size and reaches a constant value only for samples having as small a volume as $0.1 \times 0.1 \times 0.2$ mm. Hence, for observation of correct line widths very small samples were necessary. Magnetic field measurements were made with a nuclear magnetic probe, as explained in the next section.

RESULTS ON SINGLE CRYSTALS

Single crystals of (I) diphenyl picryl hydrazyl, (II) *p*-anisyl nitrogen oxide, and (III) 2-(phenyl nitrogen oxide)-2-methyl pentane-4-one-oxime-*N*-phenyl ether, structural formulas for which are shown in Table I, have been measured. The measuring procedure was similar to that employed by Kikuchi and Cohen.³ During measurements the crystals were mounted on a

TABLE I. Observed spectroscopic splitting factors and line width for some single crystals of organic free radicals.

Radical	g factor	Line widths in gauss	
		at 36 kMc/sec	at 75 kMc/sec
(I)  1,1-diphenyl-2-picryl hydrazyl	$g_{11} = 2.0035$ $g_{\perp} = 2.0043$	4	10
(II)  di- <i>p</i> -anisyl nitrogen oxide	$g_{11} = 2.0095$ $g_{\perp} = 2.0035$	14	30
(III)  2-(phenyl nitrogen oxide)-2-methyl pentane-4-one-oxime- <i>N</i> -phenyl ether	$g_x = 2.0042$ $g_y = 2.0064$ $g_z = 2.0083$	12	23

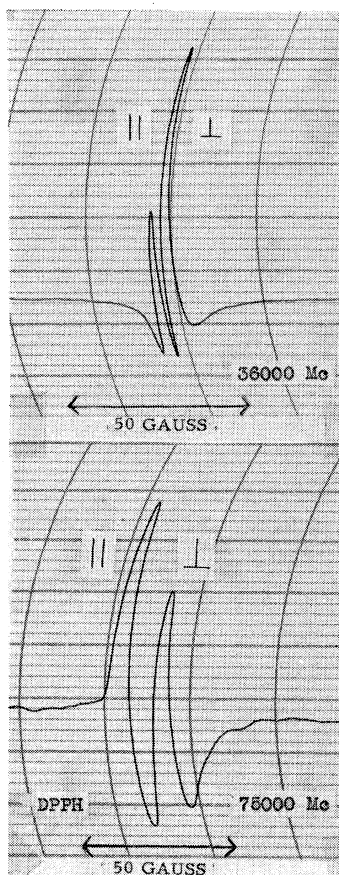


FIG. 2. Resonances at 36 and 75 kMc/sec of two DPPH crystals mounted with their axes parallel and perpendicular to the magnetic field.

Pyrex rod and inserted into the cavity in such a way that they could be rotated to orientations in which the longest axis was perpendicular, or parallel, to the magnetic field. The observed shift in resonance value is due to anisotropy in the g factor for the crystals. For accurate measurements two crystals were mounted together on the rod; the resonance line of one of the crystals served as marker for the other. The resonance lines of two DPPH crystals, one mounted parallel and one mounted perpendicular to the magnetic field, are shown in Fig. 2. The distance between these lines was calibrated with a recording that gives six hyperfine structure lines from Mn^{2+} as an impurity in ZnS. The difference in g value for both lines is 0.0008, which corresponds closely to the difference in g value measured at 24 kMc/sec by Hutchison, Pastor, and Kowalsky.²

To obtain the absolute g factor at these frequencies we calibrated the magnetic field with a nuclear resonance probe containing D_2O . The samples of D_2O and the free radical were made as nearly as possible of the same size and were placed alternately in the same spot within the magnetic field. The g factors for DPPH agree satisfactorily with those measured² at 24 kMc/sec. Once calibrated in this way, the DPPH resonances were used as a secondary standard for measurement of the g factors of the other two radicals.

Figure 3 gives the perpendicular DPPH marker against the lines from radical (II) in perpendicular and parallel orientations. This yields an anisotropy of 0.0060 in the g factor of this radical, with g values of 2.0035 and 2.0095 for the perpendicular and parallel orientations. Radical (III) does not have axial symmetry, but instead has three different g values along orientations perpendicular to each other. Figure 4 shows these lines against the perpendicular DPPH marker. The various g values are given in Table I. No dependence of g upon observation frequency was evident within the accuracy of the measurements, $\sim \pm 0.0002$ at 36 and 75 kMc/sec.

The g factors for the first two radicals listed in Table I have axial symmetry. Although the detailed crystal structure is not known, it seems reasonable that the axis of magnetic symmetry is along the $-N-N-$ bond in the DPPH and along the NO bond in the other radicals. The resonance in single crystals of the first two radicals (hyperfine structure absent) is described by the spin Hamiltonian:

$$\mathcal{H} = g_{\parallel} \beta H_z S_z + g_{\perp} \beta (H_x S_x + H_y S_y), \quad (2)$$

with the effective spin $S = \frac{1}{2}$ and with the g_{\parallel} and g_{\perp} values listed in Table I. The resonance frequency is:

$$\nu = g \beta H / h, \quad (3)$$

where

$$g = (g_{\parallel}^2 \cos^2 \theta + g_{\perp}^2 \sin^2 \theta)^{\frac{1}{2}}, \quad (4)$$

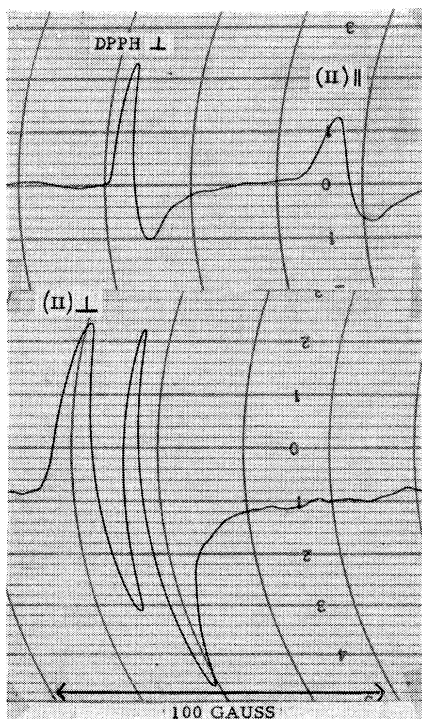


FIG. 3. Resonances at 75 kMc/sec for parallel and perpendicular orientations in H of crystals of radical (II) (*p*-anisyl nitrogen oxide) compared with that for the perpendicular orientation of DPPH.

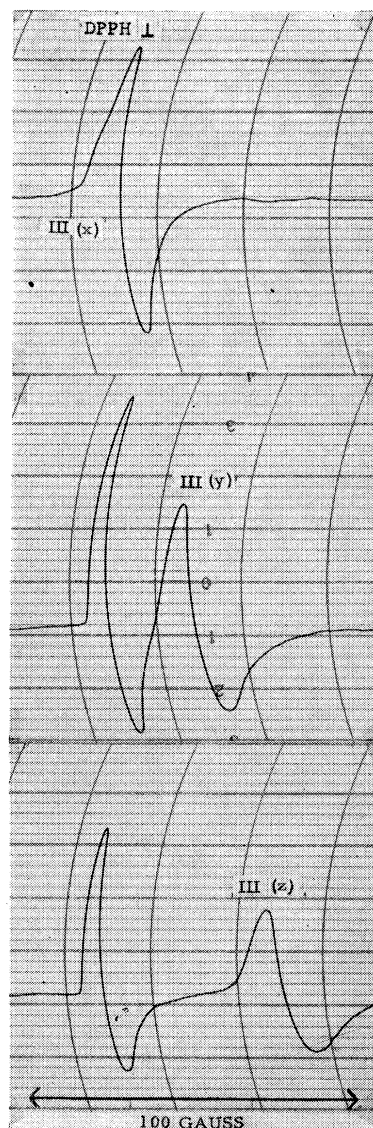


FIG. 4. Resonances at 75 kMc/sec of a single crystal of radical (III) (Table I) for orientations of the different principal magnetic axes x , y , and z along H as compared with that for the perpendicular orientation of DPPH.

where θ is the angle between H and the symmetry axis.

As might be anticipated from its complex chemical formula, the magnetic symmetry of the third radical listed in Table I is lower than that of the first two. Its resonance in the single crystal is described by the spin Hamiltonian:

$$\mathcal{H} = \beta (g_x H_x S_x + g_y H_y S_y + g_z H_z S_z), \quad (5)$$

where $S = \frac{1}{2}$ and where g_x , g_y , and g_z are the g values along the principal axes of magnetic susceptibility. The experimentally determined values of g_x , g_y , and g_z are listed in Table I. The resonant frequency for an arbitrary orientation is given by Eq. (3), with

$$g = (g_x^2 \cos^2 \theta_x + g_y^2 \cos^2 \theta_y + g_z^2 \cos^2 \theta_z)^{\frac{1}{2}}, \quad (6)$$

where θ_x , θ_y , and θ_z are the angles between H and the respective axes— x , y , and z .

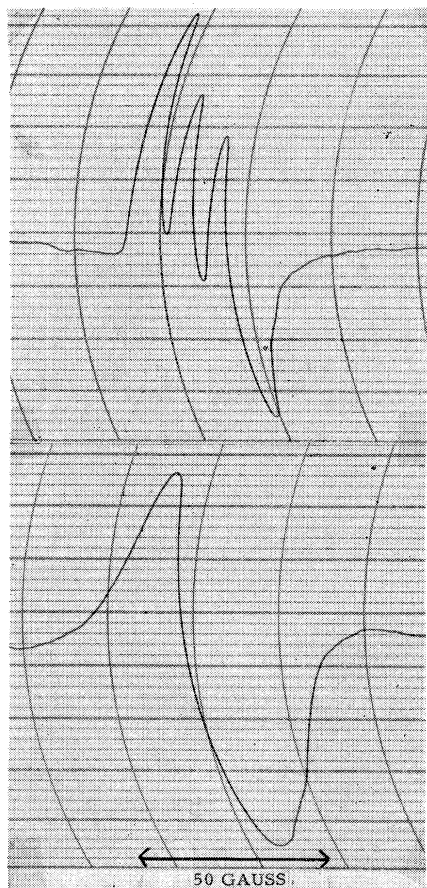


FIG. 5. Resonance of radical (II) (Table I) in dilute benzene solution (upper curve) and in the same solution when frozen (lower curve).

Diamagnetism of the associated rings, which has been suggested⁸ as a possible cause of the anisotropy earlier found in DPPH, appears to be much too small to account for the observed anisotropy of the other two radicals of this study, if indeed it can account for the smaller anisotropy found in DPPH. If the effective induced dipole-to-electron distance is assumed equal to the radius of the benzene ring plus the $-C-N-$ distance, an anisotropy of 0.1 gauss per benzene ring due to ring diamagnetization is estimated at 75 kMc/sec for a g factor of 2. This procedure of course gives only an approximation of the actual benzene ring effects; but, since the observed orientation effects are a hundred to five hundred times larger in these free radicals, it does not appear likely that the ring diamagnetization is the principal cause of the anisotropy. It seems more probable that the anisotropy in g for each radical arises primarily from a residual spin orbit coupling. This interpretation is in agreement with the nuclear couplings found in dilute solutions, which suggest that the odd electron density is mostly concentrated on a two-atom group. The fact that the hyperfine structure is elimi-

nated by exchange interaction in the solid crystals does not mean that the greater concentration of electronic spin is not still on the $-N-N-$ or $-NO$ group, nor does it mean necessarily that the residual spin orbit coupling would also be erased by the exchange interaction.

It may be seen from Table I that the width of the individual line is approximately proportional to the observation frequency (or magnetic field). This is as expected from Eq. (1) if the line width arises mainly from a slight difference in effective g values for different radicals in the crystal, caused perhaps by such conditions as vibrational motions and slight imperfections in the crystal structure.

HYPERFINE STRUCTURE

In dilute liquid solutions the anisotropy in g is averaged out by the tumbling motions of the radicals. In addition, the exchange interaction which averages out the nuclear hyperfine structure of the concentrated crystals is broken down by separation of the radicals so that their electronic wave functions no longer overlap. The isotropic terms in the nuclear coupling can then lead to an observable hyperfine structure. Under these conditions the spin Hamiltonian is:

$$\mathcal{H} = g\beta\mathbf{H} \cdot \mathbf{S} + \sum_i A_i \mathbf{S} \cdot \mathbf{I}_i \quad (7)$$

The nuclear interactions are usually small as compared with $g\beta H$, and the Back-Goudsmit effect (strong-field case) is observed. The line frequencies are then given by:

$$h\nu = g\beta H + \sum_i A_i M_{I_i} \quad (8)$$

where A_i is the coupling constant of the i th nucleus in the radical and M_{I_i} is the nuclear magnetic quantum number.

The hyperfine structure of DPPH in dilute solutions has previously been found.² Five components were observed. This qualitative fact alone shows that the unpaired spin is associated equally with the two nitrogens of the radical. The magnetic coupling constant A to each N is 10 gauss.

In the present work we have found that the resonances of radicals (II) and (III) (listed in Tables I and II) when in dilute benzene solution have triplet hyperfine structures arising from interaction of the electron spin with only one N^{14} nucleus. See Figs. 5

TABLE II. Hyperfine structure of radicals in benzene solutions at 36 kMc/sec.

	Radical ^a		
	I	II	III
Number of components	5	3	3
Width of components (gauss)	8	8	9
Total hyperfine spacing (gauss)	40	25	27
N^{14} coupling constant (gauss)	10	12.5	13.5
Width when frozen (gauss)	~10	~25	~25

^a For names and formulas see Table I.

and 6 and Table II. The coupling constant is almost the same in the two radicals. No evidence for splitting or significant broadening of the lines by proton moments is found. It seems reasonable, therefore, that the unpaired spin is associated mainly with a single NO group in each radical. Although it probably exchanges between the N and O (as it does between the two N's of DPPH), because O has the greater electronegativity the odd electron probably spends more time on the N than on the O. This is in agreement with the slightly larger coupling constant for N^{14} of the NO than for one of the N's in DPPH on which the odd electron spends at most only half the time. Since in the liquid solutions the anisotropic components of the nuclear couplings are averaged out by the tumbling motions of the radicals, the observed couplings must therefore arise from *s* orbital contributions of the nitrogens to the wave functions of the odd electrons in each radical.

Marked changes in the resonance of the dilute solutions (which were all about 0.001 mole percent in benzene) were observed to occur upon freezing of these solutions. See Figs. 5, 6, and 7. In radicals (II) and (III) the hyperfine structure was smeared out into a broad, unresolved resonance approximately equal to, or broader than, the total hyperfine span. This can be attributed to a cessation of tumbling motions upon freezing, and thus to a restoration of the anisotropy in *g*

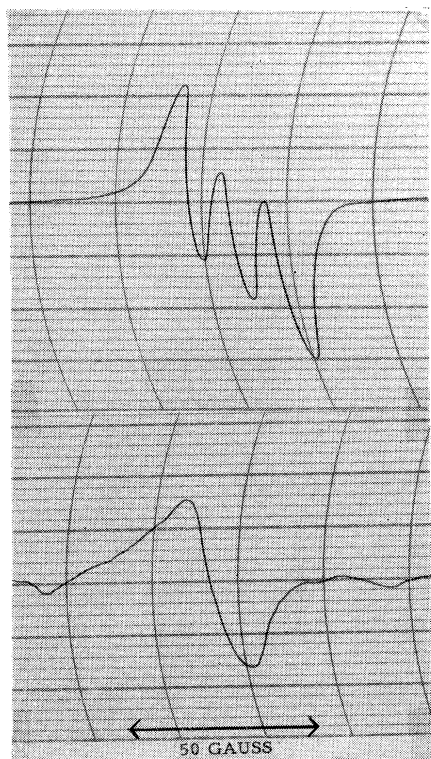
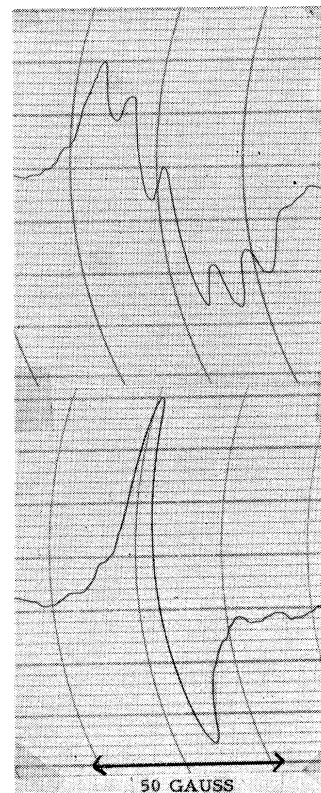


FIG. 6. Resonance of radical (III) (Table I) in dilute benzene solution (upper curve) and in the same solution when frozen (lower curve).

FIG. 7. Resonance of DPPH in dilute benzene solution (upper curve) and in the same solution when frozen (lower curve).



and any orientation-dependent nuclear interactions. An interesting difference occurred, however, for DPPH. Upon freezing, the hyperfine structure of DPPH collapsed into a single line of total width significantly less than that of the hyperfine spread (see Fig. 7) and approximately equal to that observed for the concentrated polycrystalline DPPH. One possible explanation of this phenomenon is a phase separation of the DPPH and the benzene upon freezing so that the DPPH is concentrated in small crystallites in which exchange interaction, which averages out the hyperfine structure, can occur. A more questionable interpretation is erasure of the hyperfine structure through a super-exchange interaction involving the benzene molecules in the frozen solutions.

We made some preliminary studies of radicals (II) and (III) in mixed solvents of benzene and polystyrene. The concentration of the free radical was held constant, and the viscosity of the solution was changed by varying the relative amounts of benzene and polystyrene. As the viscosity of the solution was increased by this process, the structure of the resonance was observed to change from the resolved triplet hyperfine structure to the broad, unresolved resonance observed for the completely frozen solution. We think that the onset of broadening corresponds to a cessation of the tumbling motions of the radicals which in the less viscous solutions average out the anisotropic components of the resonance.

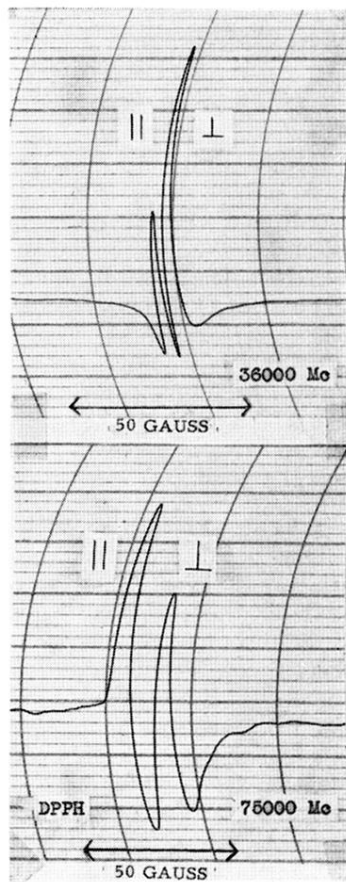


FIG. 2. Resonances at 36 and 75 kMc/sec of two DPPH crystals mounted with their axes parallel and perpendicular to the magnetic field.

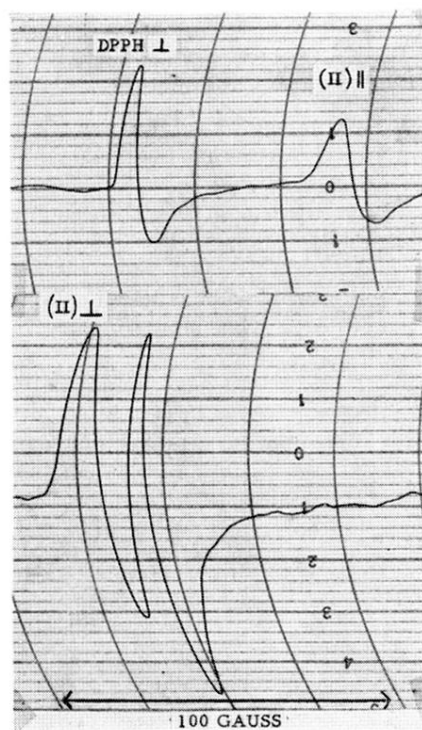
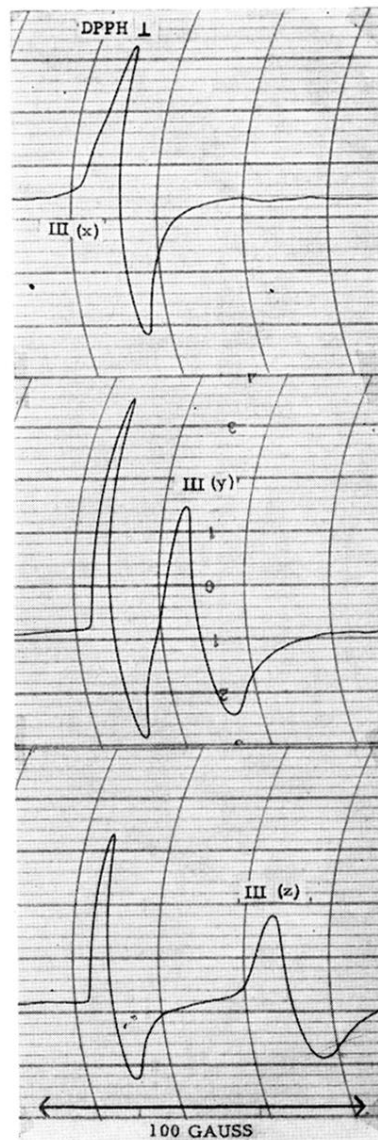


FIG. 3. Resonances at 75 kMc/sec for parallel and perpendicular orientations in H of crystals of radical (II) (p -anisyl nitrogen oxide) compared with that for the perpendicular orientation of DPPH.

FIG. 4. Resonances at 75 kMc/sec of a single crystal of radical (III) (Table I) for orientations of the different principal magnetic axes x , y , and z along H as compared with that for the perpendicular orientation of DPPH.



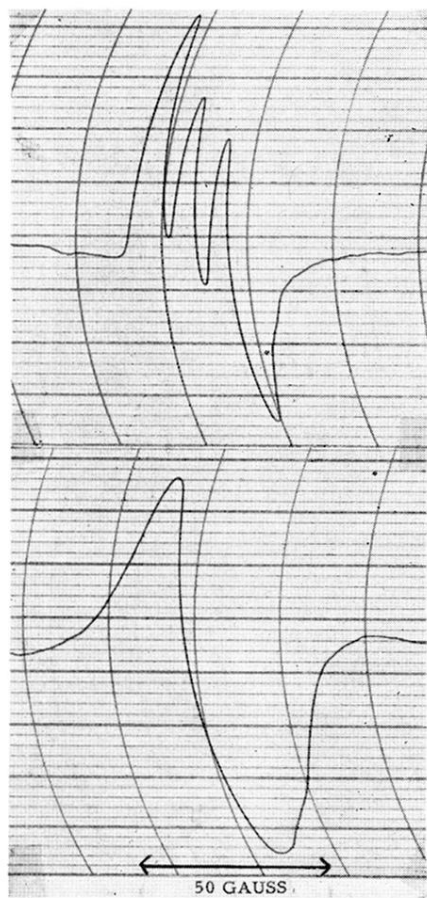


FIG. 5. Resonance of radical (II) (Table I) in dilute benzene solution (upper curve) and in the same solution when frozen (lower curve).

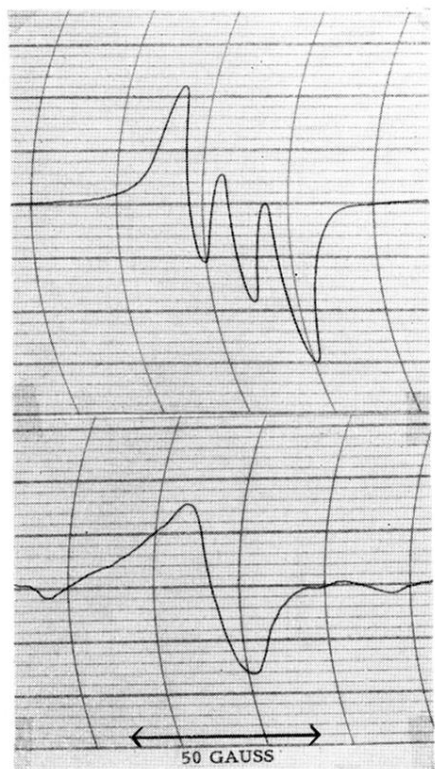


FIG. 6. Resonance of radical (III) (Table I) in dilute benzene solution (upper curve) and in the same solution when frozen (lower curve).

FIG. 7. Resonance of DPPH in dilute benzene solution (upper curve) and in the same solution when frozen (lower curve).

